Received: 29 June 2020 | Revised: 3 September 2020 | Accepted: 7 September 2020

DOI: 10.1002/jrs.5997

SPECIAL ISSUE - RESEARCH ARTICLE

Journal of RAMAN SPECTROSCOPY WILEY

Dynamics of deterministically positioned single-bond surface-enhanced Raman scattering from DNA origami assembled in plasmonic nanogaps

Rohit Chikkaraddy | **Vladimir A Turek** | **Qianqi Lin** | **Jack Griffiths** | **Bart de Nijs** | **Ulrich F Keyser** | **Jeremy J Baumberg**

NanoPhotonics Centre, Cavendish Laboratory, Department of Physics, University of Cambridge, Cambridge, UK

Correspondence
Rohit Chikkaraddy and Jeremy J. Baumberg, NanoPhotonics Centre, Cavendish Laboratory, Department of Physics, University of Cambridge, JJ Thompson Avenue, CB3 0HE Cambridge, UK.
Email: rc621@cam.ac.uk; jjb12@cam.ac.uk

Funding information
Engineering and Physical Sciences Research Council (EPSRC), Grant/Award Numbers: EP/G060649/1, EP/L027151/1, EP/G037221/1, EPSRC NanoDTC; Isaac Newton Trust; Leverhulme Trust; Trinity College, University of Cambridge

Abstract

We study the dynamics of single bonds through the surface-enhanced Raman scattering (SERS) from single SERS-marker molecules containing a distinctive single alkyl bond. Assembly of the nanogaps and positioning of single molecules inside the electromagnetic hotspot are precisely controlled using DNA origami constructs. The observed SERS intensities and their spectral wandering, together with electromagnetic simulations, all confirm the role of picocavities in this nanogap geometry in allowing observation of SERS signatures from individual vibrating bonds. The strong electromagnetic field around each picocavity and the transient binding of the SERS-marker molecule reveal significant modifications to bond vibrations and selection rules over time.

KEYWORDS

adatoms, DNA origami, plasmonics, SERS, single molecule

1 | INTRODUCTION

The transport of light, heat, and charge through single molecules has immense implications in nanotechnology for building electronic and nanophotonic devices. Central to these transport phenomena is their dependence on molecular vibrations. Optical tools to measure vibrational fingerprints of molecules at the single-copy limit are so far limited to metal nanogaps. Nanogaps formed between two metal surfaces can amplify electromagnetic (EM) fields by orders of magnitude ($E/E_0 > 100$) and confine optical fields to volumes less than 100 nm^3. Such confined EM hotspots are sufficient to surface-enhanced Raman scattering (SERS) from individual molecular vibrations with weak scattering cross-sections less than 10^{-29} cm^2 [1]. However, a major challenge has been to obtain nanogaps with uniform fields and then position molecules accurately inside these tiny hotspots.[2,3]

Nonreliable gap sizes and molecular assemblies have hindered quantitative single-molecule SERS studies to a great extent. Large variations in spectral intensity and spectral wandering are often observed and have been associated with molecular diffusion, chemical reactions, photothermal heating, and local charging.[4–12] Although these discussions largely focus on the molecule being probed, it is also important to consider the dynamic restructuring of metal nanogaps through local surface diffusion of metal adatoms. Careful consideration of how an adatom binds to the molecule, along with molecular dynamics, will have great

interest for building robust diodes, transistors, switches, and memory devices.[13–15] Current state-of-the-art synthesis methods for single-molecule plasmonic devices generally suffer from inherent randomness and/or low device yield, for instance, seen in surface chemical functionalization,[16] host-guest chemistry,[17,18] electrostatic trapping,[19] or utilizing capillary forces in solvent evaporation[20–22] or placement by probes in scanning tunneling or atomic force microscopes(AFM).

Motivated by these challenges in both molecular assembly and understanding, here we place single molecules with a characteristic bond vibration deterministically within a plasmonic nanogap and study their SERS dynamics.

2 | METHODS

The detailed sample assembly with DNA origami (DNAo) spacers and their optical characterization as nanoparticle-on-mirror (NPoM) constructs (see below) is described in our previous work.[23] In brief, each Au substrate was functionalized with folded DNAo templates by immersing the samples in DNAo solution with 1-mM $MgCl_2$, 0.5× TBE buffer. AuNPs functionalized with 5′thiol-modified 20× poly-T strands were allowed to hybridize for at least 30 min with the origami previously assembled onto Au substrate. Once fully assembled, the substrate is rinsed with Milli-Q water and blown dry with nitrogen. The surface coverage density of AuNPs is kept sufficiently low to allow for single AuNP characterization. It is important to note that the AuNPs are not aggregated in solution. The resulting dry samples are placed under a microscope equipped with simultaneous SERS and dark-field characterization at the single NP level. SERS is collected in a backscattering geometry with excitation from a 0.9-NA, 100× air-immersion objective lens.

2.1 | Finite-domain time difference simulation

The NPoM geometry is modeled with Lumerical FDTD Solutions to numerically solve the EM fields in 3D. A faceted AuNP is modeled as a truncated sphere with a diameter of 80 nm on top of an infinite dielectric sheet of $n = 2.0$ and thickness 4.5 nm and using a lower AuNP circular facet diameter of 20 nm. Underneath this sheet, a thick gold layer is placed to replicate the experimental NPoM geometry. The dielectric function of gold is taken from Johnson and Christy.[24] A 1-nm global mesh is used with an added 0.2-nm local mesh at the junction to improve accuracy. The nanoparticle is illuminated with a *p*-polarized plane wave (total-field scattered-field source) from an angle of incidence of 90°. To obtain scattering spectra, the scattered light at each wavelength is collected within a cone of half-angle 55° based on the numerical aperture of the objective. The SERS enhancement factor (*EF*) is estimated as $EF = E^2_{\lambda_p} \times E^2_{3100cm^{-1}}$, E^2_i obtained from near-field enhancements at the respective wavelengths.

2.2 | Density function theory calculation

DBCO molecules were modeled with and without binding to single gold atoms to calculate Raman and infrared (IR) spectra. Gas-phase geometry optimizations and wavenumber calculations were performed with no symmetry restrictions. B3LYP hybrid functional and def2SVP basis set were used, in combination with Grimme's D3 dispersion correction with Becke-Johnson dumping.[25] The UltraFine intergration grid was used to enhance accuracy of calculations. All density function theory (DFT) calculations were carried out with the Gaussian09 program package.[26] All computational spectra were scaled by a factor of 0.92 to match with experiment.

3 | RESULTS

We assemble NPoM[23,27–29] constructs (Figure 1a) using deoxyribonucleic-acid origami (DNAo) technology and extend it to place individual molecules at the sites of interest. As previously demonstrated,[23,30] DNAo is a powerful tool to reliably and consistently construct such architectures. Optical-frequency charge oscillations in faceted gold nanoparticles (AuNP) placed above a metal surface in this NPoM geometry provide enhanced EM hotspots in the nanoparticle-mirror junction resulting from the Coulomb coupling of induced nanoparticle dipoles and their image charges. In these nanogaps, the molecule of interest is then positioned with nm accuracy.[23,27]

In comparison with previous work where resonant dye molecules are used to probe single-molecule SERS,[1,31–36] here we use a nonresonant dibenzoclyclooctane (DBCO) molecule as the Raman probe (Figure 1b). A DNA staple strand functionalized with DBCO at the 5′ end is used to precisely position the molecule at the center of nanogap (Figure S1). This molecule contains a single alkyne (—C≡C—) bond with a distinctive vibrational signature in the Raman-silent region of DNA strands. This is an important consideration as it is otherwise lost in a profusion of vibrations arising from the DNA itself. The —C≡C— is in the nonplanar octane ring giving rise to strain in the DBCO which is used for azide reactions in click

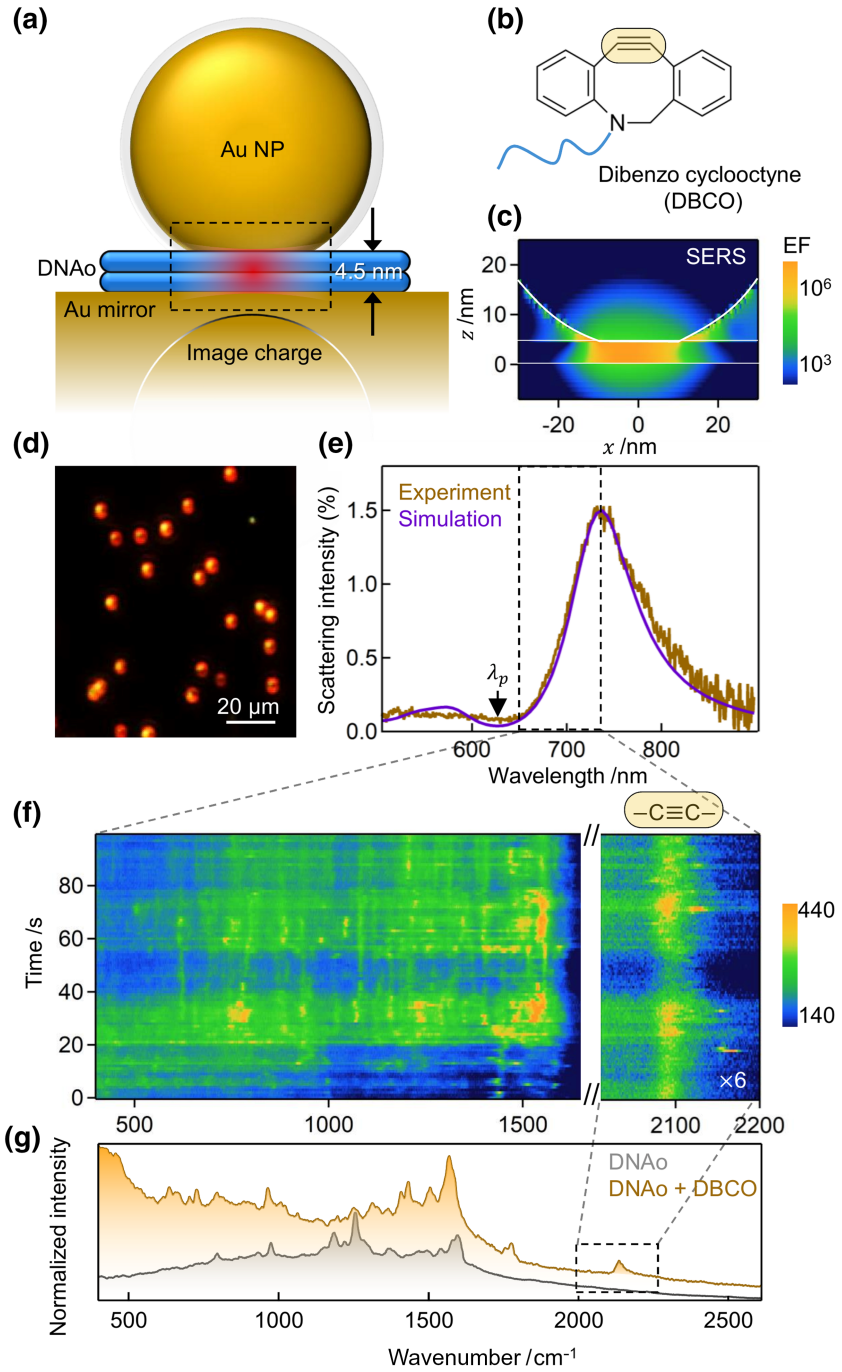

FIGURE 1 Nanoparticle-on-mirror (NPoM) construct with a single DBCO molecule in the gap. (a) Schematic of NPoM with a faceted nanoparticle on DNA origami (DNAo) plates in the gap. (b) Chemical structure of DBCO molecule positioned in the nanogap with DNAo (chemical structure of linker between DBCO and DNA staple is provided in Figure S1). Characteristic —C≡C— bond vibration of DBCO at 2,100 cm^{-1} is highlighted in yellow. (c) Full-wave 3D simulation of electromagnetic (EM) surface-enhanced Raman scattering (SERS) enhancement for NPoM geometry at the Raman shifted —C≡C— bond vibration (with λ_p=633 nm). (d) Optical dark-field image of NPoM sample—each bright red spot corresponds to an individual NPoM. (e) Scattering spectra of an individual NPoM obtained experimentally (brown) and from EM simulation (purple). Arrow indicates λ_p pump for SERS and collection region is marked dashed. (f) Time-series SERS spectra obtained from DNAo with DBCO molecules from individual NPoMs at a pump intensity of 100 μW/μm^2. The unique vibrational region of DBCO is labeled as —C≡C—. (g) Time averaged SERS spectra of DNAo, compared with that of DNAo containing single DBCO labels, in individual NPoM gaps (time-series SERS spectra of DNAo are provided in Figure S2)

chemistry.[37] Note that —C≡C— bond stretching has weak IR absorption associated with a tiny change in dipole strength, making it harder to detect in tip-based near-field IR absorption methods. Our assembled structure here provides SERS EFs of several millions (Figure 1c), whereas only a single DBCO is present in each NPoM gap.

Scattering from individual NPoM constructs measured using dark-field microscopy (Figure 1d) exhibits a characteristic coupled mode resonance around 735 nm (Figure 1e) specific to the nanogap geometry.[38] Full-wave simulations are performed to validate this with experimentally obtained input parameters[23] perfectly matching with the experimentally observed spectrum (Figure 1e, purple curve), confirming the reliability of simulated near-fields and estimated EF values. It is important to notice that the simulated EF of 10^6 is not sufficient to observe single-molecule SERS and that greater than 90% of the EM field in the gap is polarized along the *z*-direction normal to the metal facets.[29,39]

However, when an individual NPoM is pumped at λ_p = 633 nm and plasmon-enhanced SERS spectra are collected in the region 400 to 2,200 cm^{-1}, we observe SERS signals from the single —C≡C— stretch at 2,100 cm^{-1}. This can only be explained by including an

additional local amplification of EM fields which is created by the picocavity formed when Au atoms are pulled out of the facets.[40] For picocavities forming at the mirror substrate,[41] the EM hotspot does not reach the —C≡C— as it assembles near the AuNP at the top DNAo plate. Time-series spectra with 1-s integration time further reveal the dynamics (Figure 1f). The —C≡C— stretch exhibits strong intensity fluctuations which have some correlation with SERS signals from the large number of DNAo vibrational bands in its fingerprint region 500 to 1,600 cm^{-1}. In this region, it is extremely hard to differentiate the vibrational bands associated with DNA from those of DBCO (Figure 1g).

To understand the dynamics of single molecules, we thus focus on a small region of higher wavenumbers (2,000-2,500 cm^{-1}) around the —C≡C— stretch (Figure 2a). These spectra are decomposed into peak and background by fitting them with Gaussian and linear background contributions. The intensity fluctuations observed from the time-series SERS spectra of different individual NPoMs at 2,100 cm^{-1} confirm that the single-molecule origin of the signal and corroborates the picocavity events. Unprocessed spectra and background fits are provided in the Figure S3. Irrespective of the intrinsic variability of the nanoparticle size (<5%) and shape, greater than 50% of observed NPoMs show a Raman peak around 2,100 cm^{-1}, indicating high yield of assembly. The intensity of the —C≡C— bond vibrations exhibit greater than 5× variation across multiple NPoM constructs, indicating flexible linkage of DBCO inside the DNAo and thus different —C≡C— bond orientations inside the gap, giving counts $<10^3$ mW/μm^2/s. Optimized collection geometries could further improve the photon yield to $>10^5$ mW/μm^2/s, allowing us to observe the dynamics at millisecond resolution.[42]

The —C≡C— bond vibrations show spectral wandering of $\Delta\bar{\nu}$ apprximately 5 to 10 cm^{-1} on timescales of 1 s (Figure 2b). These shifts are 2 × smaller than the smallest linewidth observed in the time series spectra. Although the —C≡C— intensity fluctuates by more than 100%, no correlation is found with the background intensity variations (Figure 2c). This implies that the molecular fluctuations originate from local EM and chemical modifications and that the mechanisms for background and peak intensity variations are different.[43,44] Local melting of the DNAo or changes in —C≡C— bond orientation are unlikely to contribute to these intensity variations, as the estimated change in temperature for the pump power used is less than 1° C.

4 | DISCUSSION

The local amplification of EM fields from a picocavity is estimated using classical full-wave simulations evidencing the strong field around a single Au adatom (Figure 3a).

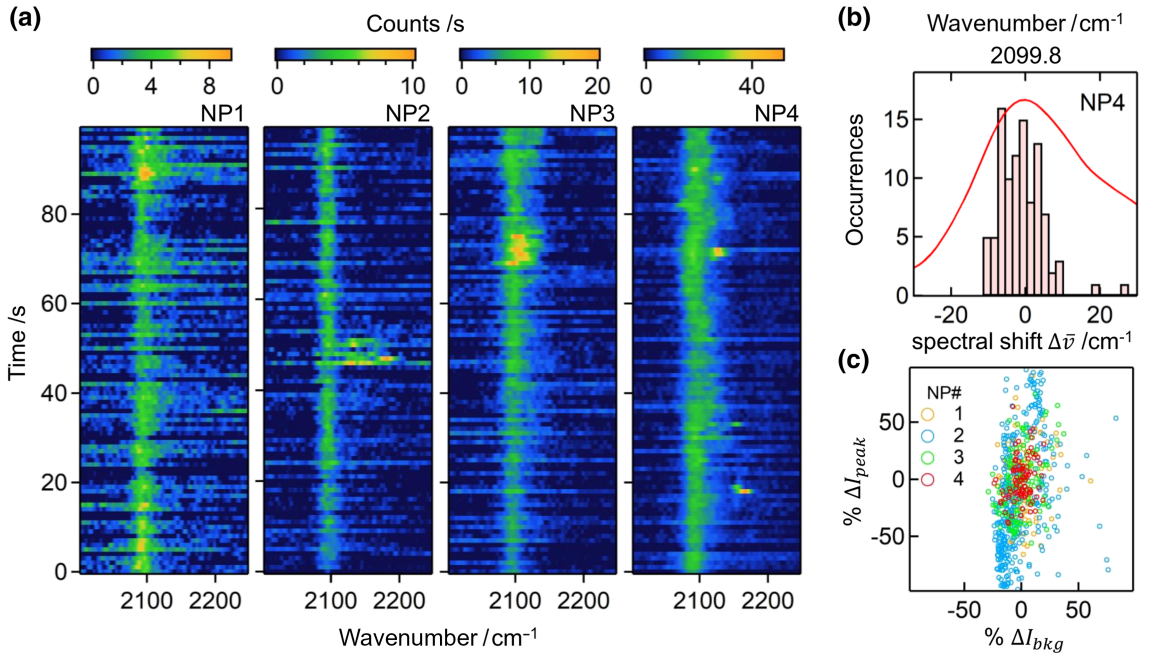

FIGURE 2 Surface-enhanced Raman scattering (SERS) dynamics of a single —C≡C— vibration. (a) Time-series SERS spectra of single DBCO molecules from four different nanoparticle-on-mirror (NPoM) gaps. (b) Spectral wandering of —C≡C— vibration extracted from NP4. Solid red curve is time averaged spectrum. (c) Peak intensity variation of —C≡C— bond vibrations, which has no correlation with the SERS background intensity fluctuations

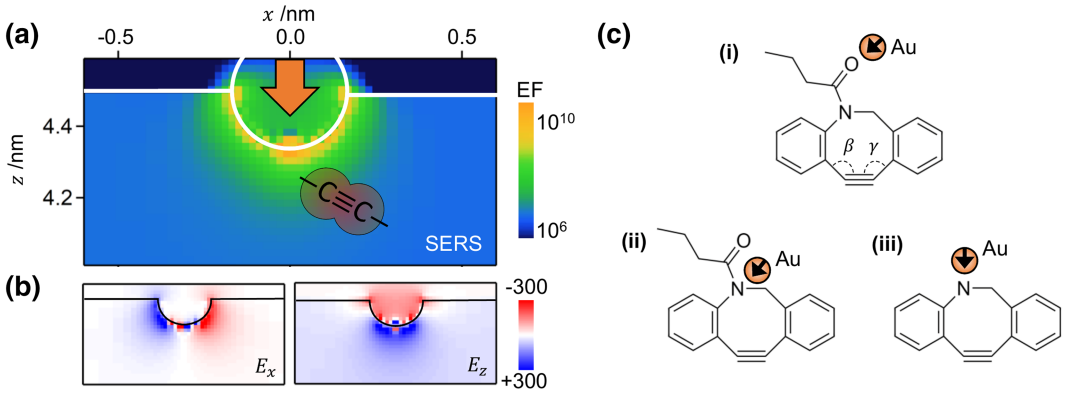

(d) Results analysed from DFT for different Au-bound DBCO molecule

Configurations of Au binding	Change in vibrational energy	Change in Raman cross-section	$\beta - \gamma$
(i)	-9 cm^{-1}	10%	3°
(ii)	-150 cm^{-1}	6%	Changes triple bond to -C=C=C-
(iii)	-9 cm^{-1}	12%	2°

FIGURE 3 Adatom-induced electromagnetic (EM) enhancement on surface-enhanced Raman scattering (SERS). (a) Classical enhancement EF for SERS at 2,100 cm^{-1} mode in nanoparticle-on-mirror (NPoM) when single gold atom is pulled out of AuNP facet. Strong increase in local field strength is observed in comparison with fields without adatom (Figure 1c). (b) Simulated real components of E_x and E_z fields at 713 nm (≡2,100 cm^{-1}). (c) Different configurations of Au binding to DBCO molecules used for density function theory (DFT) calculations (full optimized structure and analysis provided in Figures S4–S6). For non-Au bound DBCO, linear deformation $\beta - \gamma$ is 1°. (d) Tabulated estimates from DFT for different configurations shown in (c)

This has been shown to match full quantum calculations.[45] The additional EM field at the adatom tip now boosts the EF from 10^6 to greater than 10^{10}, allowing single-molecule SERS from gaps as small as 4.5 nm. The strong field gradients around the —C≡C— bond can further modify the selection rules [40, 46] (Figure 3b). This is occasionally observed as multiple extra Raman peaks in the same 2,100 cm^{-1} region, with spectral shifts from the —C≡C— stretch of greater than 10 cm^{-1} (Figure 2a, NP4).

Chemical perturbations due to the binding of Au adatoms on the DBCO affect the —C≡C— strength and strain in the octane ring. This is estimated using DFT calculations by considering different configurations of Au atom binding to this DBCO molecule (Figure 3c). There are two potential binding sites for Au: (i) binding to the —C═O group of the amide bond near the octane ring and (ii) binding to the nitrogen in the octane ring. Both these influence the —C≡C— bond strength, Raman cross-section, and strain in the octane ring. The reconfiguration of this nonplanar octane ring on binding of Au is estimated from the difference between β and γ angles around the —C≡C— bond (Figure 3c*i*). The DFT extracted values are tabulated in Figure 3d. The possibility of Au binding to nitrogen is unlikely as it is expected to either destroy the —C≡C— bond or break the functional alkyl chain as shown in configuration (iii). The more likely site is thus the Au attaching to the —C═O group which perturbs the —C≡C— bond strength by −9 cm^{-1} which is in reasonable agreement with the experimental data ($\Delta\bar{\nu}$ 5–10 cm^{-1}). The intensity fluctuations predicted are, however, much smaller than observed, though a full model for predicted intensities from picocavities is not yet available. We also note that the influence of the large number of nearby DNAo base pairs and phosphate backbones with high local concentrations of $MgCl_2$ ions remains unclear and needs further investigation.

To conclude, we show SERS dynamics from individual fully nonresonant DBCO molecules deterministically positioned in plasmonic nanogaps. From SERS analysis, it is evident that the local EM field controlled by the picocavities enhance the EF by four orders of magnitude in addition to nanocavity fields, allowing the probing of vibrational dynamics from a single —C≡C— bond. The strong modification observed in the —C≡C— stretch including the presence of multiple peaks at high wavenumbers indicates the role of chemical environment. Our results should reinitiate the debate about light-induced chemical effects on SERS.

ACKNOWLEDGEMENTS

We acknowledge support from EPSRC grants EP/G060649/1, EP/L027151/1, EP/G037221/1, and EPSRC NanoDTC. R. C. acknowledges support from Trinity College, University of Cambridge. B. d. N. acknowledges support from the Leverhulme Trust and Isaac Newton Trust in the form of an Early Career Fellowship.

CONFLICTS OF INTEREST

The authors declare no competing financial interest.

DATA AVAILABILITY STATEMENT

Source data can be found at https://doi.org/10.17863/CAM.57071

ORCID

Rohit Chikkaraddy https://orcid.org/0000-0002-3840-4188
Qianqi Lin https://orcid.org/0000-0001-7578-838X
Jeremy J Baumberg https://orcid.org/0000-0002-9606-9488

REFERENCES

[1] D.-K. Lim, K.-S. Jeon, H. M. Kim, J.-M. Nam, Y. D. Suh, *Nat. Mater.* **2010**, *9*, 60.
[2] J. Langer, D. J. de Aberasturi, J. Aizpurua, R. A. Alvarez-Puebla, B. Auguié, J. J. Baumberg, G. C. Bazan, S. E. J. Bell, A. Boisen, A. G. Brolo, J. Choo, D. Cialla-May, V. Deckert, L. Fabris, K. Faulds, F. J. G. de Abajo, R. Goodacre, D. Graham, A. J. Haes, C. L. Haynes, C. Huck, T. Itoh, M. Käll, J. Kneipp, N. A. Kotov, H. Kuang, E. C. Le Ru, H. K. Lee, J.-F. Li, X. Y. Ling, S. A. Maier, T. Mayerhöfer, M. Moskovits, K. Murakoshi, J.-M. Nam, S. Nie, Y. Ozaki, I. Pastoriza-Santos, J. Perez-Juste, J. Popp, A. Pucci, S. Reich, B. Ren, G. C. Schatz, T. Shegai, S. Schlücker, L.-L. Tay, K. G. Thomas, Z.-Q. Tian, R. P. Van Duyne, T. Vo-Dinh, Y. Wang, K. A. Willets, C. Xu, H. Xu, Y. Xu, Y. S. Yamamoto, B. Zhao, L. M. Liz-Marzán, *ACS Nano* **2020**, *14*, 28.
[3] J. Aizpurua, H. Arnolds, J. Baumberg, I. Bruzas, R. Chikkaraddy, M. Chisanga, P. Dawson, V. Deckert, I. Delfino, B. de Nijs, G. D. Martino, J. Edel, H. Fleming, S. Gawinkowski, F. Giorgis, R. Goodacre, D. Graham, M. Hardy, C. Heck, S. Heeg, K. Hewitt, L. Jamieson, A. Keeler, A. Królikowska, C. Kuttner, N. Lidgi-Guigui, C. Lightner, J. Lombardi, S. Mahajan, N. M. Sabanés, J.-F. Masson, N. S. Mueller, H. Muhamadali, K. Murakoshi, J. Popp, M. Porter, S. Reich, G. Schatz, Z.-Q. Tian, A. Tripathi, R. V. Duyne, X. Wang, A. Wark, K. Willets, M. Willner, *Faraday Discuss* **2017**, *205*, 291.
[4] C.-Y. Li, S. Duan, J. Yi, C. Wang, P. M. Radjenovic, Z.-Q. Tian, J.-F. Li, *Sci. Adv.* **2020**, *6*, eaba6012.
[5] K.-D. Park, E. A. Muller, V. Kravtsov, P. M. Sass, J. Dreyer, J. M. Atkin, M. B. Raschke, *Nano Lett.* **2016**, *16*, 479.
[6] J. Guan, C. Jia, Y. Li, Z. Liu, J. Wang, Z. Yang, C. Gu, D. Su, K. N. Houk, D. Zhang, X. Guo, *Sci. Adv.* **2018**, *4*, eaar2177.
[7] E. A. Pozzi, A. B. Zrimsek, C. M. Lethiec, G. C. Schatz, M. C. Hersam, R. P. Van Duyne, *J. Phys. Chem. C* **2015**, *119*, 21116.
[8] D. P. dos Santos, M. L. A. Temperini, A. G. Brolo, *Acc. Chem. Res.* **2019**, *52*, 456.
[9] E. C. Le Ru, P. G. Etchegoin, *Annu. Rev. Phys. Chem.* **2012**, *63*, 65.
[10] H.-K. Choi, K. S. Lee, H.-H. Shin, J.-J. Koo, G. J. Yeon, Z. H. Kim, *Acc. Chem. Res.* **2019**, *52*, 3008.
[11] B. de Nijs, F. Benz, S. J. Barrow, D. O. Sigle, R. Chikkaraddy, A. Palma, C. Carnegie, M. Kamp, R. Sundararaman, P. Narang, O. A. Scherman, J. J. Baumberg, *Nat. Commun.* **2017**, *8*, 994.
[12] P. P. Patra, R. Chikkaraddy, R. P. N. Tripathi, A. Dasgupta, G. V. P. Kumar, *Nat. Commun.* **2014**, *5*, ncomms5357.
[13] J. Lee, H. Chang, S. Kim, G. S. Bang, H. Lee, *Am. Ethnol.* **2009**, *121*, 8653.
[14] C. Jia, A. Migliore, N. Xin, S. Huang, J. Wang, Q. Yang, S. Wang, H. Chen, D. Wang, B. Feng, Z. Liu, G. Zhang, D.-H. Qu, H. Tian, M. A. Ratner, H. Q. Xu, A. Nitzan, X. Guo, *Science* **2016**, *352*, 1443.
[15] T. A. Su, H. Li, M. L. Steigerwald, L. Venkataraman, C. Nuckolls, *Nat. Chem.* **2015**, *7*, 215.
[16] S. K. Kufer, E. M. Puchner, H. Gumpp, T. Liedl, H. E. Gaub, *Science* **2008**, *319*, 594.
[17] R. Chikkaraddy, B. de Nijs, F. Benz, S. J. Barrow, O. A. Scherman, E. Rosta, A. Demetriadou, P. Fox, O. Hess, J. J. Baumberg, *Nature* **2016**, *535*, 127.
[18] D. O. Sigle, S. Kasera, L. O. Herrmann, A. Palma, B. de Nijs, F. Benz, S. Mahajan, J. J. Baumberg, O. A. Scherman, *J. Phys. Chem. Lett.* **2016**, *7*, 704.
[19] M. Krishnan, N. Mojarad, P. Kukura, V. Sandoghdar, *Nature* **2010**, *467*, 692.
[20] C. U. Hail, C. Höller, K. Matsuzaki, P. Rohner, J. Renger, V. Sandoghdar, D. Poulikakos, H. Eghlidi, *Nat. Commun.* **2019**, *10*, 1880.
[21] M. Hu, F. S. Ou, W. Wu, I. Naumov, X. Li, A. M. Bratkovsky, R. S. Williams, Z. Li, *J. Am. Chem. Soc.* **2010**, *132*, 12820.
[22] Y. Zheng, A. H. Soeriyadi, L. Rosa, S. H. Ng, U. Bach, J. J. Gooding, *Nat. Commun.* **2015**, *6*, 8797.
[23] R. Chikkaraddy, V. A. Turek, N. Kongsuwan, F. Benz, C. Carnegie, T. van de Goor, B. de Nijs, A. Demetriadou, O. Hess, U. F. Keyser, J. J. Baumberg, *Nano Lett.* **2018**, *18*, 405.
[24] P. B. Johnson, R. W. Christy, *Phys. Rev. B* **1972**, *6*, 4370.
[25] S. Grimme, S. Ehrlich, L. Goerigk, *J. Comput. Chem.* **2011**, *32*, 1456.
[26] M. J. Frisch, G. W. Trucks, H. B. Schlegel, G. E. Scuseria, M. A. Robb, J. R. Cheeseman, G. Scalmani, V. Barone, G. A. Petersson, H. Nakatsuji, X. Li, M. Caricato, A. V. Marenich, J. Bloino, B. G. Janesko, R. Gomperts, B. Mennucci, H. P. Hratchian, J. V. Ortiz, A. F. Izmaylov, J. L. Sonnenberg, D. Williams-Young, F. Ding, F. Lipparini, F. Egidi, J. Goings, B. Peng, A. Petrone, T. Henderson, D. Ranasinghe, V. G. Zakrzewski, J. Gao, N. Rega, G. Zheng, W. Liang, M. Hada, M. Ehara, K. Toyota, R. Fukuda, J. Hasegawa, M. Ishida, T. Nakajima, Y. Honda, O. Kitao, H. Nakai, T. Vreven, K. Throssell, J. A. Montgomery Jr., J. E. Peralta, F. Ogliaro, M. J. Bearpark, J. J. Heyd, E. N. Brothers, K. N. Kudin, V. N. Staroverov, T. A. Keith, R. Kobayashi, J. Normand, K. Raghavachari, A. P. Rendell,

J. C. Burant, S. S. Iyengar, J. Tomasi, M. Cossi, J. M. Millam, M. Klene, C. Adamo, R. Cammi, J. W. Ochterski, R. L. Martin, K. Morokuma, O. Farkas, J. B. Foresman, D. J. Fox, *Gaussian09 Revision E01* **2009**.

[27] N. Kongsuwan, A. Demetriadou, R. Chikkaraddy, F. Benz, V. A. Turek, U. F. Keyser, J. J. Baumberg, O. Hess, *ACS Photonics* **2018**, *5*, 186.

[28] J. J. Baumberg, J. Aizpurua, M. H. Mikkelsen, D. R. Smith, *Nat. Mater.* **2019**, *18*, 668.

[29] M. J. Horton, O. S. Ojambati, R. Chikkaraddy, W. M. Deacon, N. Kongsuwan, A. Demetriadou, O. Hess, J. J. Baumberg, *Proc. Natl. Acad. Sci.* **2020**, *117*, 2275.

[30] V. V. Thacker, L. O. Herrmann, D. O. Sigle, T. Zhang, T. Liedl, J. J. Baumberg, U. F. Keyser, *Nat. Commun.* **2014**, *5*, ncomms4448.

[31] J.-H. Lee, M.-H. You, G.-H. Kim, J.-M. Nam, *Nano Lett.* **2014**, *14*, 6217.

[32] H. Lee, J.-H. Lee, S. M. Jin, Y. D. Suh, J.-M. Nam, *Nano Lett.* **2013**, *13*, 6113.

[33] S. Simoncelli, E.-M. Roller, P. Urban, R. Schreiber, A. J. Turberfield, T. Liedl, T. Lohmüller, *ACS Nano* **2016**, *10*, 9809.

[34] P. Kühler, E.-M. Roller, R. Schreiber, T. Liedl, T. Lohmüller, J. Feldmann, *Nano Lett.* **2014**, *14*, 2914.

[35] B. Shen, V. Linko, K. Tapio, S. Pikker, T. Lemma, A. Gopinath, K. V. Gothelf, M. A. Kostiainen, J. J. Toppari, *Sci. Adv.* **2018**, *4*, eaap8978.

[36] E. Pibiri, P. Holzmeister, B. Lalkens, G. P. Acuna, P. Tinnefeld, *Nano Lett.* **2014**, *14*, 3499.

[37] C. R. Becer, R. Hoogenboom, U. S. Schubert, *Angew. Chem., Int. Ed.* **2009**, *48*, 4900.

[38] R. Chikkaraddy, X. Zheng, F. Benz, L. J. Brooks, B. de Nijs, C. Carnegie, M.-E. Kleemann, J. Mertens, R. W. Bowman, G. A. E. Vandenbosch, V. V. Moshchalkov, J. J. Baumberg, *ACS Photonics* **2017**, *4*, 469.

[39] N. Kongsuwan, A. Demetriadou, M. Horton, R. Chikkaraddy, J. J. Baumberg, O. Hess, *ACS Photonics* **2020**, *7*, 463.

[40] F. Benz, M. K. Schmidt, A. Dreismann, R. Chikkaraddy, Y. Zhang, A. Demetriadou, C. Carnegie, H. Ohadi, B. de Nijs, R. Esteban, J. Aizpurua, J. J. Baumberg, *Science* **2016**, *354*, 726.

[41] C. Carnegie, J. Griffiths, B. de Nijs, C. Readman, R. Chikkaraddy, W. M. Deacon, Y. Zhang, I. Szabó, E. Rosta, J. Aizpurua, J. J. Baumberg, *J. Phys. Chem. Lett.* **2018**, *9*, 7146.

[42] M. Kamp, B. de Nijs, N. Kongsuwan, M. Saba, R. Chikkaraddy, C. A. Readman, W. M. Deacon, J. Griffiths, S. J. Barrow, O. S. Ojambati, D. Wright, J. Huang, O. Hess, O. A. Scherman, J. J. Baumberg, *Natl. Acad. Sci. 117*, 14819. https://doi.org/10.1073/pnas.1920091117

[43] C. Carnegie, M. Urbieta, R. Chikkaraddy, B. de Nijs, J. Griffiths, W. M. Deacon, M. Kamp, N. Zabala, J. Aizpurua, J. J. Baumberg, *Nat. Commun.* **2020**, *11*, 682.

[44] J. Mertens, M.-E. Kleemann, R. Chikkaraddy, P. Narang, J. J. Baumberg, *Nano Lett.* **2017**, *17*, 2568.

[45] M. Urbieta, M. Barbry, Y. Zhang, P. Koval, D. Sánchez-Portal, N. Zabala, J. Aizpurua, *ACS Nano* **2018**, *12*, 585.

[46] O. S. Ojambati, W. M. Deacon, R. Chikkaraddy, C. Readman, Q. Lin, Z. Koczor-Benda, E. Rosta, O. A. Scherman, J. J. Baumberg, *ACS Photonics* **2020**, https://doi.org/10.1021/acsphotonics.0c00732

SUPPORTING INFORMATION

Additional supporting information may be found online in the Supporting Information section at the end of this article.

How to cite this article: Chikkaraddy R, Turek VA, Lin Q, et al. Dynamics of deterministically positioned single-bond surface-enhanced Raman scattering from DNA origami assembled in plasmonic nanogaps. *J Raman Spectrosc*. 2021;52:348–354. https://doi.org/10.1002/jrs.5997